Biomineralisation performance of bacteria isolated from a landfill in China

RAJASEKAR, Adharsh, WILKINSON, Stephen, SEKAR, Raju, BRIDGE, Jonathan <http://orcid.org/0000-0003-3717-519X>, MEDINA-ROLDAN, Eduardo and MOY, Charles K.S

Biomineralisation performance of bacteria isolated from a landfill in China

Adharsh Rajasekar[a,*], Stephen Wilkinson[b], Raju Sekar[c], Jonathan Bridge[d], Eduardo-Medina Roldan[e], Charles K.S.Moy[a]

[a] Department of Civil Engineering, Xi'an Jiaotong-Liverpool University, Suzhou 215123, Jiangsu, China

[b] Department of Civil Engineering, University of Wolverhampton, Wolverhampton WV1 1LY, United Kingdom

[c] Department of Biological Sciences, Xi'an Jiaotong-Liverpool University, Suzhou 215123, Jiangsu, China

[d] Department of the Natural and Built Environment, Sheffield Hallam University, Sheffield S1 1WB, United Kingdom

[e] Department of Environmental Science, Xi'an Jiaotong-Liverpool University, Suzhou 215123, Jiangsu, China

[*]Corresponding author:

Adharsh Rajasekar

evolution.adharsh@gmail.com

+8618261444592

Abstract

We report an investigation of microbially-induced carbonate precipitation by seven indigenous bacteria isolated from a landfill in China. Bacterial strains were cultured in a medium supplemented with 25 mM calcium chloride and 333 mM urea. The experiments were carried out at 30 °C for 7 days with agitation by a shaking table at 130 rpm. Scanning Electron Microscopic (SEM) and X-ray diffraction (XRD) analyses showed variations in calcium carbonate polymorphs and mineral composition induced by all bacterial strains. The amount of carbonate precipitation was quantified by titration. The amount of carbonate precipitated in the medium varied among isolates with the lowest being *Bacillus aerius rawirorabr15* (LC092833) precipitating around 1.5 times more carbonate per unit volume than the abiotic (blank) solution. *Pseudomonas nitroreducens* szh_asesj15 (LC090854) was found to be the most efficient, precipitating 3.2 times more carbonate than the abiotic solution. Our results indicate that bacterial carbonate precipitation occurred through ureolysis and suggest that variations in carbonate crystal polymorphs and rates of precipitation were driven by strain-specific differences in urease expression and response to the alkaline environment. These results and the method applied provide benchmarking/screening data for assessing the bioremediation potential of indigenous bacteria for containment of contaminants in landfills.

Keywords: Biomineralisation, Indigenous bacteria, Landfill, *Bacillus*, *Pseudomonas*, SEM

Introduction

The potential of microbial species to stimulate precipitation of carbonates is well known in various natural environments, including soils, geological formations, oceans, and saline lakes (Boquet et al. 1973). This bio-mediated process is known as microbially induced carbonate precipitation (MICP). The ability of these bacteria to precipitate carbonates has been widely studied (Rivadeneyra et al. 2006, Sanchez-Roman et al. 2007, Rivadeneyra et al. 2000, Rivadeneyra et al. 2004, Han et al. 2013, Kang et al. 2014a). Both active and passive mechanisms have been proposed to explain how bacteria mediate the precipitation process (Hammes and Verstraete 2002, Silva-Castro et al. 2013). The most widely-studied of these, particularly in respect of potential engineering applications, is urease hydrolysis by organisms involved in the nitrogen cycle (Rivadeneyra et al. 2006, Gorospe et al. 2013, Achal and Pan 2014, Dhami et al. 2014). While urease activity is common in bacteria, the amount and rate of carbonate precipitation varies among species and genera and is dependent on local environmental conditions (Zamarreňo et al. 2009). A range of factors may account for this variation: (i) rate of urea hydrolysis related to use of urea as an energy source; (ii) the alkalinity of the local environment, which affects carbonate speciation and $CaCO_3$ solubility; (iii) the affinity of the bacterial cell surfaces for Ca^{2+} ions, which can create micro-scale supersaturation of Ca^{2+} in the vicinity of cells; potentially leading to (iv) nucleation and crystal growth where carbonate is also sufficiently saturated.

In previous studies, carbonate-precipitating bacteria have been isolated from contaminated and disturbed environments such as mine tailing soils (Achal and Pan 2014), caves (Rusznyak et al. 2012), and highways (Kang et al. 2014a). Landfills are complex microbial

systems inhabited by bacteria that remediate or degrade toxic compounds (Staley et al. 2011). We have recently shown, for an urban landfill in China, a diverse population of organisms including genera known to have biomineralisation potential (Rajasekar et al. 2018). Stimulating carbonate precipitation in indigenous bacteria already adapted to the biochemically-harsh environmental conditions of a landfill is a potentially cost-, materials- and energy-efficient alternative to geotechnical or geoenvironmental engineering approaches for control of landfill leachate. Indigenous microbes could be used for modification of groundwater flow, or contaminant/heavy metal immobilization by co-precipitation as substitute ions for calcium or simple trapping in cemented pore spaces (Ivanov and Chu 2008, Miot et al. 2009, Kang et al. 2014b, Amidi and Wang 2015). For example, (Kang et al. 2014a) and (Ma et al. 2009) have used biomineralisation to trap heavy metals such as cadmium. Achal et al. (2012a) utilised this technique to immobilise arsenic and (Kang et al. 2015) assessed the containment of lead.

Access to many landfill and other controlled sites for extended investigation of contamination and remediation techniques *in situ* is often logistically difficult but sampling for water quality and microbiological analysis is more feasible. Thus, many more biomineralisation studies have been implemented in the lab than in the field. *In situ* biomineralisation to achieve geotechnical and remediation engineering objectives is still in its early stages and the priority remains identification of MICP-capable organisms capable of existing under specific site conditions (like landfills) and characterising their biomineralisation potential (Kang et al. 2015, Kang et al. 2014a, Fujita et al. 2004, Achal et al. 2012b, Kang et al. 2014b).

This study aims to establish a rapid laboratory protocol designed to identify, using cultures isolated from landfill water samples (i) the presence of carbonate-precipitating bacteria within the indigenous community; (ii) the degree of variability in bioremediation potential among species; and (iii) the characteristics of MICP mechanisms demonstrated by the isolates. The results offer well-constrained, benchmarking data for further studies of the potential of indigenous microbes for techniques such as bioremediation or contaminants containment in extreme contaminated environments such as landfills.

Materials and Methods

Sampling and Storage

The landfill (31°14′18.31”N 120°33’3.09”E) is located in Suzhou, Jiangsu, China. The regional limestone geology is described in full in (Rajasekar et al., 2018) and the landfill receives a mix of incinerator ash and raw municipal waste. Water samples were collected in triplicate using a handheld peristaltic pump through sterile PVC tubing into sterile high-density polyethylene (HDPE) sealable plastic bottles and stored at 4°C prior to bacterial isolation. Groundwater samples were collected from boreholes on the perimeter of the landfill at 4 m below surface, approximately 1.9 m below the local water table. ‘Fresh’ leachate was collected directly from a pipe that drains the body of the landfill. ‘Raw’ leachate was collected from an engineered leachate pond.

Isolation and identification of bacterial isolates

A detailed investigation of the bacterial consortia at the case study landfill site was carried out using Illumina MiseqPE250 next-generation sequencing as reported previously by (Rajasekar et al. 2018).

For this study, bacterial isolates were obtained using the following procedure. Raw and fresh leachate samples with serial dilutions were spread onto nutrient agar (hopebio, Qingdao, China) and incubated at 30°C for 24 hours until visible colonies were obtained. The bacterial isolates were purified by repeated streaking and then transferred into nutrient broth (BD, Difco™, USA). The spread plate method was also used for bacterial isolation from an undiluted 100µl groundwater aliquot and the isolates were purified by repeated streaking. The cells were harvested and pellets directly transferred to the bead columns for DNA extraction. The genomic DNA was extracted using PowerSoil® DNA isolation kit (MO BIO, USA) following the manufacturer's instructions. The 16S rRNA genes were amplified using PCR with 10 mM concentration of 27F and 1492R primers (Muyzer et al. 1993). A final volume of 50 µL was used in the PCR assay, which contains 10X PCR buffer (5 µL), 10 mmol/L dNTPs (1 µL), 25 mmol/L $MgCl_2$ (4 µL), forward and reverse primers 10mM each (2µL), Taq polymerase (2 U), DNA template (1 µL), and 37 µL of double-distilled water. The PCR cycling conditions were as follows: initial denaturation at 94 °C for 4 minutes followed by 30 cycles of denaturation at 94 °C for 1 minute, annealing at 55 °C for 35 seconds, extension for 1 minute at 72 °C; after 30 cycles final extension at 72 °C for 10 minutes. The PCR products were verified by agarose gel (1.5% wt/v) electrophoresis and purified using a PCR purification kit (Axygen®, CA, USA). The purified PCR products were sequenced at a sequencing facility (Sangon Biotech Co Ltd) in Shanghai, China using 27F primer. The partial sequences were compared using BLAST queuing system (Altschul et al. 1990) to identify their closest relatives and tentative phylogenetic positions. The sequences were later submitted to DNA Data Bank of Japan (DDBJ) for acquisition of

unique accession numbers for the sequences (LC090023, LC092830-33, and LC090854-55).

Urease activity assay

The isolates were tested for urease activity on urea agar media using the method described by (Hammes et al. 2003). All the isolates tested positive for urease enzyme. This was confirmed after 5 days of incubation at 28°C.

Biomineralisation assay

Biomineralisation media consisted of 25 mM calcium chloride solution (purity ≥98%), 333 mM of urea solution (purity ≥ 97 %) and 0.8 g of nutrient broth (BD, Difco™, USA) per 150 ml consistent with published methods used in previous MICP studies (Kang et al. 2014a, Muynck et al. 2010b, Helmi et al. 2016, Muynck et al. 2010a, Achal and Pan 2014). The initial pH was 9.1 and adjust to pH 7.5 with HCl. Calcium chloride solution was autoclaved and filter-sterilized to avoid any contamination before mixing. Urea solution was only filter-sterilized to avoid denaturing of the urea at high temperatures. Two mL of the bacterial culture (grown overnight in nutrient broth at 30 °C for 24 hours) were added to 150 mL of the biomineralisation media and incubated in a rotary shaker at 120 rpm for 7 days at 30 °C. Sterile biomineralisation media without bacterial isolates was used as a blank control. The pH of the bacterial and abiotic control solutions were recorded using a Suntex TS1 pH meter once every 24 hours. The pH was checked under a laminar hood to avoid any potential contamination. After 7 days of incubation, the solution was vacuum filtered through a sterile 0.6 µm Whatman® membrane filter (Whatman®, USA). Each filter paper was placed in a separate sterile Petri dish and air dried at 37°C for 24 hours for subsequent analyses. All incubations were carried out in triplicate.

156 ***Scanning Electron Microscopy (SEM)***

157 Fragments of residue from each filter paper were transferred onto double-sided carbon tape
158 affixed to standard 5 mm electron microscope stubs for imaging using an Hitachi TM3000
159 scanning electron microscope. Five mm stubs were used to allow easy transportation and
160 storage of samples for future observation and an adaptor was used to allow the stubs to be
161 inserted on top of the Hitachi TM3000 stage. The samples were imaged uncoated, under
162 relatively low vacuum conditions. Images were taken at magnifications between 400× and
163 1500× to allow the identification of crystals formed due to biomineralisation. Due to the
164 low magnification used, no charging errors were recorded during imaging.

165 ***X-ray powder diffraction (XRD) analysis***

166 A powder sample was created by scraping reside from the filter papers using a sterile razor
167 blade directly onto the sample holder of the X-ray diffractometer (Advanced D8, Bruker,
168 Germany). The upper surface was then carefully flattened using a glass slide. The sample
169 holder was rotated during measurement to ensure good sampling of the crystal lattices
170 within the powder sample.

171 ***Carbonate titration analysis***

172 The total carbonate present in the residue on each filter was quantified using titration
173 following the method of (Maulood et al. 2012). The amount of residue (grams) that's
174 deposited on the filter paper after filtration influences the value of carbonate precipitation
175 since all the residue that's deposited on the paper is used for titration. The residue is
176 weighed before the titration to calculate the amount of carbonate precipitated during the
177 process.

178 **Results**

Identification of bacterial isolates by 16S rRNA gene sequencing

Five strains isolated from landfill leachate belonged to members of genus *Bacillus.* Among these, two were isolated from raw leachate and three from fresh leachate samples (Table 1). The bacteria isolated from landfill groundwater belonged to the genera *Pseudomonas* and *Sphingopyxis*. Two indigenous bacterial strains isolated from the landfill groundwater were identified as *Pseudomonas nitroreducens* szh_asesj15 (LC090854) and *Sphingopyxis* sp. szh_adharsh (LC090855) by 16S rRNA gene sequencing (Table 1). *Pseudomonas* belongs to γ-Proteobacteria and has commonly been found in landfills (Kalwasinska and Burkowska 2013). *Sphingopyxis* belongs to α-Proteobacteria, and members of this genus are extremely resistant towards soil contamination such as that from high heavy metal concentrations (Choi et al. 2010).

pH variation with time during biomineralisation assay

Figure 1 A shows the change in pH as a function of time during the biomineralisation assays. Landfill leachate isolates (Fig. 1A) experienced a lag phase during the first 24 hours in which pH remained steady, while in experiments with isolates from groundwater the pH started to increase immediately (Fig. 1B). Steady rise in pH was observed in all assays from 24 h through 144 h, with the highest value obtained by *Sphingopyxis* isolated from landfill groundwater (mean pH 10±0.1. The pH of medium with *Bacillus licheniformis* SZH2015_A was found to be decreasing after 120 hours, which was not observed in any of the other bacterial isolates (Fig. 1 A). In the abiotic control, pH increased steadily from pH 7.5 to pH 8.5 ($\pm$0.033) from 0-144 h (Figure 1 B).

SEM analysis

Figures 2 and 3 illustrate the range of calcium carbonate crystal morphologies observed in

SEM. Spherical crystals were ubiquitous in all bacterial experiments but rare or absent in abiotic controls, where rhombohedral crystals dominated. Morphological distinction was observed in certain crystals from bacterial isolates (Fig. 3 A & B). In some cases, evidence was observed of direct bacteria-crystal contacts. Fig. 3B shows elongate pits on the surface of a crystal. Fig. 2E shows the growth of micro crystals on the surface of a calcite crystal. Two different types of crystal fusion were observed in Fig. 2A and Fig. 3A which has the potential of resulting in the formation of one larger crystal.

XRD analysis

XRD spectra indicated the primary component of all the precipitates was Calcite, although Vaterite was detected in some cases as well.

Carbonate quantification

Comparison between the urease activities of the isolates was determined using carbonate titration. The isolate with the highest pH value was not found to have the highest carbonate precipitation (Fig. 6). *Pseudomonas nitroreducens* szh_asesj15 was observed to have the highest carbonate precipitation (0.88±0.2), while *Bacillus pumilus* szhxjlu2015 was observed to have the lowest carbonate precipitation (0.41 ±0.3). The blank was observed to have the lowest carbonate precipitation when compared with bacterial isolates which is expected since it has no urease activity.

Discussion

Analysis of pH in bacterial and blank solutions

The maximum pH measurements for all of the bacterial isolates exceeded that of the blank (Fig. 1 A&B). This was expected since the blank did not have the urease enzyme. The pH surge within 24 hours of the experiment observed in the leachate isolates was quite

different when compared with the groundwater isolates. Even among the leachate bacteria, pH variations could be observed. This indicated that each bacterium undergoes different rates of ureolysis for carbonate precipitation. During the first 24 hours of incubation, the pH of the *Bacillus pumilus szhxjlu2015* and *Bacillus aerius rawirorabr15* decreased from their initial pH values (Fig. 1 A). This was probably due to the different adaptation time of the bacteria to the environment for urea hydrolysis (Lian et al. 2006). Bacteria such as *Bacillus subtilis* have been shown to pump out protons through their cell walls during respiration (Mera et al. 1992). These protons will presumably occupy the negatively charged cell surface sites and lower the pH of the local environment. This early reduction in pH has also been observed by (Rivadeneyra et al. 2006, Sanchez-Roman et al. 2007). In comparison to Figs. 1 A and B shows an increase in pH from 7.5 to ~8.4 for the groundwater bacteria during the first 24 hours following inoculation into biomineralisation medium. It has been reported that certain ureolytic bacteria begin the process of urea hydrolysis within 24 hours for carbonate precipitation (Achal and Pan 2014). For the groundwater bacteria, the pH increased almost linearly over 144 hours presumably because of the consistent enzymatic hydrolysis of urea and higher CO_3^{2-} precipitation and upon depletion of the dissolved urea results in an reduction in pH (Stocks-Fischer et al. 1999).

$$CO(NH_2)_2 + H_2O \xrightarrow{\text{bacteria}} NH_2COOH + NH_3$$

$$NH_2COOH + H_2O \longrightarrow NH_3 + H_2CO_3$$

These products equilibrate in water to form bicarbonate,1mole of ammonium and hydroxide ions which give rise to pH increase

$$H_2CO_3 \longrightarrow 2H^+ + 2CO_3^{2-}$$

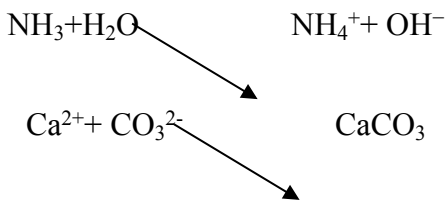

A similar trend was also observed with the bacteria isolated from leachate after 48 hours (Fig. 1 A). All the leachate bacteria are in their linear progressive state (consistent increase in pH) indicated by the bacterial enzymatic hydrolysis of urea leading to an increased production in $[OH^-]$ ions which contributes to the pH increase.

At this pH, a substantial amount of carbonate is present in the solution (the pKa of HCO_3^{2-} -CO_3^{2-} is approximately one order of magnitude higher), which in turn, in the presence of calcium ions, can lead to a supersaturation of carbonate in the solution, thereby promoting the precipitation of calcium carbonate. The forward reaction is catalysed by microbes, thus allowing the generation of a higher peak pH in the bacterial solutions in comparison to the control (Fujita et al. 2008). The reduction in pH can be explained using two chemical reactions, the precipitation of calcium carbonate and the conversion of ammonium to ammonia:

$$Ca^{2+} + HCO_3^- + OH^- \rightarrow CaCO_3 + H_2O$$

$$NH_4^+ + OH^- \rightarrow NH_{3(gas)} + H_2O$$

The pH values from this study can be explained using the theory proposed by (Sanchez-Roman et al. 2007) for ureolysis. They reported that the activity of urease is optimum at a pH of 8.5, leading to superior carbonate precipitation (Gorospe et al. 2013, Stabnikov et al. 2013, Chu et al. 2014). They indicated that the metabolic activity of the bacteria is extremely important and it varies from one bacteria to another. Each bacteria supplies the

ions necessary for the formation of the minerals, namely NH_4^+ and CO_3^{2-} for carbonates. Moreover, the appropriate microenvironment is created for precipitation, i.e. increased pH and/or ionic concentration. This increased pH environment was also observed in our study for all the bacteria. This demonstrates that bacteria are not simply heterogeneous nuclei for precipitation but are also active mediators in the process.

Furthermore, the bacterial degradation of peptones and yeast extract takes place, supplying NH_4^+ leading to an increase of pH, as observed in our experiments. The metabolic activity occurring in the media, together with the concentration of ions in the cellular envelopes, will drive local oversaturation of such ions, leading to carbonate precipitation. The pH change in the abiotic solution was also observed by (Ferris et al. 2003, Gorospe et al. 2013, Achal and Pan 2014) and it is attributed to the very slow hydrolysis of urea which is speculated to be 10^{14} slower than a biotic hydrolysis of urea.

The presence of bacteria can induce the precipitation of minerals in microenvironments by the combination of two mechanisms; (1) modifying the conditions of their surrounding environments through ureolysis and/or the concentration of ions in the bacterial cell envelope (Li et al. 2013); and (2) cell walls acting as nucleation sites for the growth of the carbonate crystals (Li et al. 2011).

Morphology of crystals in bacterial and control solutions

Previous SEM studies of carbonates formed due to MICP have identified that spherical crystal forms are commonly observed in samples containing bacteria in comparison to the normal rhombohedral crystal form (trigonal system) in non-bacterial samples (Stocks-Fischer et al. 1999, Rivadeneyra et al. 2004, Lian et al. 2006, Jimenez-Lopez et al. 2007, Sánchez-Román et al. 2011). It has been suggested that spherical crystals are a result of the

292 higher rate of crystal formation which is occurring due to the action of the ureolytic bacteria
293 (Stocks-Fischer et al. 1999). The SEM images obtained for the seven bacterial isolates also
294 showed this spherical crystal morphology (Fig. 2A, B, C, D, E; Fig 3 A and B). Very similar
295 observations have been made for the well-studied ureolytic bacteria, *Bacillus megaterium*
296 (Lian et al. 2006). Further to this, the full range of observations displayed in Fig. 2 and 3
297 indicate that the bacterial strains influence both the crystal morphology and growth patterns.
298 Similar observations have been individually reported across a range of studies for other
299 biomineralising organisms (Rivadeneyra et al. 2000, Rivadeneyra et al. 2004, Lian et al.
300 2006, Jimenez-Lopez et al. 2007). The main reason for the changes in morphology is
301 probably due to the differences in ureolysis rates influenced by the bacterial density
302 (Rodriguez-Navarro et al. 2012) and the saturation index of the solution (Bosak and
303 Newman 2005, Sanchez-Roman et al. 2007, Mitchell and Ferris 2006).
304 Fused spherical crystals were observed in *Bacillus licheniformis* SZH2015_A (Fig. 2A) &
305 *Bacillus aerius* rawirorabr15 (Fig. 2E) samples, where the spherical crystals have grown
306 together and become interlocked. Xu et al. (2015) suggested that calcium sources are highly
307 influential in the clumping or fusing of crystals. This type of crystal formation is highly
308 desirable for soil applications, as it can generate very low permeability zones within a soil
309 allowing pore necks to become sealed. At a larger scale, clumping of large numbers of
310 calcite crystals is produced by *Bacillus licheniformis* adseedstjo15 (Fig. 2E). Clumping of
311 crystals occurs when the expansion of crystals displaces and entrains smaller growing
312 crystals. This leads to the formation of an interlocking framework that enables bacteria to
313 slowly establish contact with nearby crystals surfaces and develop colonies on them (Wang
314 et al. 2013). The structure which forms is not a completely fused crystal, although it is

likely to contain fused crystals. Such structures will have the effect of reducing permeability, but not to the extent of a fully interlocking crystalline structure.

Bacterial imprints were also identified on the surface of calcite crystals for *Sphingopyxis* sp. szh_adharsh (Fig. 3B). These results suggested that the bacteria might serve as nucleation sites for calcite precipitation, which is in agreement with observations with other carbonate precipitating bacteria (Lian et al. 2006, Li et al. 2011). The bacterial cell surface could induce mineral deposition by providing nucleation sites due to ion composition on its surface (Lian et al. 2006). Ion composition is referred to as the negatively charged functional groups that are present on the bacterial cell walls which attract Ca^{2+} to induce a local supersaturation so that calcite nucleation takes place on the cell surfaces. No spherical calcite forms were observed in the blank sample (Fig. 3F).

X-Ray diffraction (XRD) analysis

XRD analysis was used to measure the composition, structure and microstructure of the crystal compounds. Calcium carbonate crystals were precipitated by all the bacterial isolates in this study (Fig. 4 & 5). Calcite and vaterite were produced in all samples. The results, especially from the use of calcium chloride, concur with the previous reports in which calcite and vaterite were produced (Gorospe et al. 2013). Zamarreňo et al. (2009) reported that precipitation of calcite and vaterite were also influenced by the bacteria and the carbonate precipitation media. To our knowledge, our study indicates that bacteria rather than calcium chloride caused differences in the morphology of calcium carbonate polymorphs (Fig. 4 & 5). This is a very important finding because it suggests that each bacteria precipitate calcium carbonate polymorphs in a slightly different way in the same media.

338

339 ***Quantification of Carbonate***

340 Titration was performed to calculate and compare the efficiency of carbonate precipitation
341 by each bacterium. The final quantities of precipitated calcium carbonate were confirmed
342 through titration with 0.5 M HCl. Previous studies have shown that urease production
343 increases the pH resulting in a superior carbonate precipitation (Achal and Pan 2014).
344 Observations in our study differ from this conclusion, as the pH of *Bacillus* sp. xjlu_herc15
345 reached a higher pH than *Pseudomonas nitroreducens* szh_asesj15. However, *Bacillus* sp.
346 xjlu_herc15 precipitated 0.8 grams of carbonate compared to *Pseudomonas nitroreducens*
347 szh_asesj15 which precipitated 0.9 grams (Fig. 6). Although *Bacillus* sp. xjlu_herc15 took
348 time to adapt to the environment in comparison to the other bacteria, it still managed to
349 precipitate a superior quantity of carbonate compared to the other five bacteria. Given that
350 pH rise is correlated with urease activity, *Bacillus* sp. xjlu_herc15 has shown to have
351 superior enzyme activity compared to other bacteria from the landfill between 48 to 144
352 hours. For all of the bacterial samples, the amount of precipitation was higher than that of
353 the abiotic (blank) solution. The variation in effectiveness ranged from 1.53 to 3.2 times
354 more $CaCO_3$ precipitation per 150 ml retained on the filter paper compared to the abiotic
355 (blank) sample (Fig. 6). No carbonate precipitation was found in the abiotic samples
356 reported by Sanchez-Roman et al. 2007, Achal and Pan 2014 but recent studies conducted
357 by Zamarreño et al. 2009a, Okyay and Rodrigues 2015 reported carbonate precipitation
358 under abiotic conditions. Okyay and Rodrigues (2015) suggested that the interaction of
359 CO_2 with the abiotic media results in the precipitation of carbonate.

Conclusions

Studies based on MICP have shown that the composition of the culture medium and pH can change the type and amount of calcium carbonate precipitated. This study focuses mainly on the biomineralisation potential of indigenous bacteria from a landfill and its surroundings. Hence, we provide strong evidence of such possibility and present data showing the precipitation performance of a range of newly identified bacterial strains. Analysis of the microbially induced calcium carbonate produced was achieved using a combination of carbonate titration, SEM and XRD methods. Each bacteria, irrelevant of their environment, influenced the morphology and amount of calcium carbonate precipitation. Bacterial strain was identified as more important than pH in terms of the amount of carbonate being precipitated by the bacteria. Even though, urease activity does promote carbonate precipitation, it does not appear to be the sole determining factor of the amount of carbonate that will be precipitated. This approach makes it ideal for biostimulation of these bacteria in the landfill for environmental remediation purposes. Therefore, the authors hope that the findings from this study will potentially lead to an optimistic implication for the design of future engineering applications involving microbially induced calcite precipitation, such as sand consolidation, soil improvement, and bioremediation.

Acknowledgements

This work was supported by grant no. PGRS-12-02-06 and RDF-13-01-06 awarded by XJTLU.

Conflict of interest

No conflict of interest declared.

383

384 **References**

385 ACHAL, V. & PAN, X. 2014. Influence of calcium sources on microbially induced
386 calcium carbonate precipitation by *Bacillus* sp. CR2. *Appl Biochem Biotechnol,* 173**,**
387 307-317.
388 ACHAL, V., PAN, X., FU, Q. & ZHANG, D. 2012a. Biomineralization based remediation
389 of As(III) contaminated soil by *Sporosarcina ginsengisoli*. *J Haz Mat,* 201-202**,**
390 178-184.
391 ACHAL, V., PAN, X. & ZHANG, D. 2012b. Bioremediation of strontium (Sr)
392 contaminated aquifer quartz sand based on carbonate precipitation induced by Sr
393 resistant *Halomonas* sp. *Chemosphere,* 89**,** 764-768.
394 AMIDI, S. & WANG, J. 2015. Surface treatment of concrete bricks using calcium
395 carbonate precipitation. *Constr Buil Mat,* 80**,** 273-278.
396 BOQUET, A.BORONAT & A.RAMOS-CORMENZANA 1973. Production of Calcite
397 (Calcium Carbonate) crystals by soil bacteria is a general phenomenon. *Nature,* 246**,**
398 527-529.
399 BOSAK, T. & NEWMAN, D. K. 2005. Microbial kinetic controls on calcite morphology
400 in supersaturated solutions. *J Sedimen res,* 75**,** 190-199.
401 CHOI, J. H., KIM, M. S., JUNG, M. J., ROH, S. W., SHIN, K. S. & BAE, J. W. 2010.
402 Sphingopyxis soli sp. nov., isolated from landfill soil. *Int J Sys Evol Microbiol,* 60**,**
403 1682-1686.
404 CHU, J., IVANOV, V., NAEIMI, M., STABNIKOV, V. & LIU, H.-L. 2014. Optimization
405 of calcium-based bioclogging and biocementation of sand. *Acta Geotechnica,* 9**,**
406 277-285.
407 DHAMI, N. K., REDDY, M. S. & MUKHERJEE, A. 2014. Synergistic Role of Bacterial
408 Urease and Carbonic Anhydrase in Carbonate Mineralization. *Appl Biochem*
409 *Biotechnol,* 172**,** 2552-2561.
410 FERRIS, F. G., V.PHOENIX, FUJITA, Y. & SMITH, R. W. 2003. Kinetics of calcite
411 precipitation induced by ureolytic bacteria at 10 to 20°C in artificial groundwater.
412 *Geochimica et Cosmochimica Acta,* 67**,** 1701-1722.

FUJITA, Y., REDDEN, G. D., INGRAM, J. C., CORTEZ, M. M., FERRIS, F. G. & SMITH, R. W. 2004. Strontium incorporation into calcite generated by bacterial ureolysis. *Geochim Cosmochim Acta,* 68**,** 3261-3270.

FUJITA, Y., TAYLOR, J. L., GRESHAM, T. L. T., DELWICHE, M. E., COLWELL, F. S., MCLING, T. L., PETZKE, L. M. & SMITH, R. W. 2008. Stimulation Of Microbial Urea Hydrolysis In Groundwater To Enhance Calcite Precipitation. *Environ sci technol,* 42**,** 3025-3032.

GOROSPE, C. M., HAN, S.-H., KIM, S.-G., PARK, J.-Y., KANG, C.-H., JEONG, J.-H. & SO, J.-S. 2013. Effects of Different Calcium Salts on Calcium Carbonate Crystal Formation by *Sporosarcina pasteurii* KCTC 3558. *Biotechnol Biopro Eng,* 18**,** 903-908.

HAMMES, F., BOON, N., VILLIERS, J. D., VERSTRAETE, W. & SICILIANO, S. D. 2003. Strain-Specific Ureolytic Microbial Calcium Carbonate Precipitation. *Appl Environ Microbiol,* 69**,** 4901-4909.

HAMMES, F. & VERSTRAETE, W. 2002. Key roles of pH and calcium metabolism in microbial carbonate precipitation. *Re/Views in Environ Sci BioTechnol,* 1**,** 3-7.

HAN, Z., YAN, H., ZHOU, S., ZHAO, H., ZHANG, Y., ZHANG, N., YAO, C., ZHAO, L. & HAN, C. 2013. Precipitation of calcite induced by Synechocystis sp. PCC6803. *W J Microbiol Biotechnol,* 29**,** 1801-1811.

HELMI, F. M., ELMITWALLI, H. R., ELNAGDY, S. M. & EL-HAGRASSY, A. F. 2016. Calcium carbonate precipitation induced by ureolytic bacteria *Bacillus licheniformis*. *Ecol Eng,* 90**,** 367-371.

IVANOV, V. & CHU, J. 2008. Applications of microorganisms to geotechnical engineering for bioclogging and biocementation of soil in situ. *Reviews in Environ Sci Bio/Technol,* 7**,** 139-153.

JIMENEZ-LOPEZ, C., JROUNDI, F., RODRÍGUEZ-GALLEGO, M., ARIAS, J. M. & GONZALEZ-MUÑOZ, M. T. 2007. Biomineralization induced by Myxobacteria. *Communicating Curr Res Educational Topics and Trends in Appl Microbiol***,** 143-154.

KALWASINSKA, A. & BURKOWSKA, A. 2013. Municipal landfill sites as sources of microorganisms potentially pathogenic to humans. *Environ Sci Processes & Impacts,* 15**,** 1078-1086.

KANG, C.-H., HAN, S.-H., SHIN, Y., OH, S. J. & SO, J.-S. 2014a. Bioremediation of Cd by Microbially Induced Calcite Precipitation. *Appl Biochem Biotechnol,* 172**,** 2907-2915.

KANG, C.-H., OH, S. J., SHIN, Y., HAN, S.-H., NAM, I.-H. & SO, J.-S. 2015. Bioremediation of lead by ureolytic bacteria isolated from soil at abandoned metal mines in South Korea. *Ecol Eng,* 74**,** 402-407.

KANG, C. H., CHOI, J. H., NOH, J., KWAK, D. Y., HAN, S. H. & SO, J. S. 2014b. Microbially induced calcite precipitation-based sequestration of strontium by *Sporosarcina pasteurii* WJ-2. *Appl Biochem Biotechnol,* 174**,** 2482-2491.

LI, W., CHEN, W.-S., ZHOU, P.-P., ZHU, S.-L. & YU, L.-J. 2013. Influence of initial calcium ion concentration on the precipitation and crystal morphology of calcium carbonate induced by bacterial carbonic anhydrase. *Chem Eng J,* 218**,** 65-72.

LI, W., LIU, L.-P., ZHOU, P.-P., CAO, L., YU, L.-J. & JIANG, S.-Y. 2011. Calcite precipitation induced by bacteria and bacterially produced carbonic anhydrase. *Curr sci,* 100**,** 502-508.

LIAN, B., HU, Q., CHEN, J., JI, J. & TENG, H. H. 2006. Carbonate biomineralization induced by soil bacterium *Bacillus megaterium*. *Geochim Cosmochim Acta,* 70**,** 5522-5535.

MA, Y., LIN, C., JIANG, Y., LU, W., SI, C. & LIU, Y. 2009. Competitive removal of water-borne copper, zinc and cadmium by a $CaCO_3$-dominated red mud. *J Haz Mat,* 172**,** 1288-1296.

MAULOOD, P. M., ESMAIL, A. O., DOHUKI, M. S. S. & DARWESH, D. A. 2012. Comparison between Calcimetric and Titrimetric Methods for Calcium Carbonate Determination. *Open J Soil Sci,* 2**,** 263-268.

MERA, M. U., KEMPER, M., DOYLE, R. & BEVERIDGE, T. J. 1992. The membrane-induced proton motive force influences the metal-binding ability of Bacillus subtilis cell walls. *Appl Environ Microbiol,* 58**,** 3837-3844.

MIOT, J., BENZERARA, K., OBST, M., KAPPLER, A., HEGLER, F., SCHADLER, S., BOUCHEZ, C., GUYOT, F. & MORIN, G. 2009. Extracellular iron biomineralization by photoautotrophic iron-oxidizing bacteria. *Appl Environ Microbiol,* 75**,** 5586-5591.

MITCHELL, A. C. & FERRIS, F. G. 2006. The Influence of *Bacillus pasteurii* on the Nucleation and Growth of Calcium Carbonate. *Geomicrobiol J,* 23**,** 213-226.

MUYNCK, W. D., BELIE, N. D. & VERSTRAETE, W. 2010a. Microbial carbonate precipitation in construction materials: A review. *Ecol Eng,* 36**,** 118-136.

MUYNCK, W. D., VERBEKEN, K., BELIE, N. D. & VERSTRAETE, W. 2010b. Influence of urea and calcium dosage on the effectiveness of bacterially induced carbonate precipitation on limestone. *Ecol Eng,* 36**,** 99-111.

MUYZER, G., WAAL, E. C. D. & UITIERLINDEN, A. G. 1993. Profiling of Complex Microbial Populations by Denaturing Gradient Gel Electrophoresis Analysis of Polymerase Chain Reaction-Amplified Genes Coding for 16S rRNA. *Appl Environ Microbiol,* 59**,** 695-700.

OKYAY, T. O. & RODRIGUES, D. F. 2015. Biotic and abiotic effects on CO2 sequestration during microbially-induced calcium carbonate precipitation. *FEMS Microbiol Ecol,* 91**,** 1-13.

RAJASEKAR, A., RAJU, S., MEDINA-ROLDAN, E., BRIDGE, J., K.S.MOY, C. & WILKINSON, S. 2018. Next-generation sequencing showing potential leachate influence on bacterial communities around a landfill in China. *Can J Microbiol*.

RIVADENEYRA, M. A., DELGADO, G., SORIANO, M., RAMOS-CORMENZANA, A. & DELGADO, R. 2000. Precipitation of carbonates by Nesterenkonia halobia in liquid media. *Chemosphere,* 41**,** 617-624.

RIVADENEYRA, M. A., MARTÍN-ALGARRA, A., SÁNCHEZ-NAVAS, A. & MARTÍN-RAMOS, D. 2006. Carbonate and Phosphate Precipitation by Chromohalobacter marismortui. *Geomicrobiol J,* 23**,** 1-13.

RIVADENEYRA, M. A., PARRAGA, J., DELGADO, R., RAMOS-CORMENZANA, A. & DELGADO, G. 2004. Biomineralization of carbonates by Halobacillus trueperi in solid and liquid media with different salinities. *FEMS Microbiol Ecol,* 48**,** 39-46.

RUSZNYAK, A., AKOB, D. M., NIETZSCHE, S., EUSTERHUES, K., TOTSCHE, K. U., NEU, T. R., FROSCH, T., POPP, J., KEINER, R., GELETNEKY, J., KATZSCHMANN, L., SCHULZE, E. D. & KUSEL, K. 2012. Calcite biomineralization by bacterial isolates from the recently discovered pristine karstic herrenberg cave. *Appl Environ Microbiol,* 78**,** 1157-1167.

SANCHEZ-ROMAN, M., RIVADENEYRA, M. A., VASCONCELOS, C. & MCKENZIE, J. A. 2007. Biomineralization of carbonate and phosphate by moderately halophilic bacteria. *FEMS Microbiol Ecol,* 61**,** 273-284.

SÁNCHEZ-ROMÁN, M., ROMANEK, C. S., FERNÁNDEZ-REMOLAR, D. C., SÁNCHEZ-NAVAS, A., MCKENZIE, J. A., PIBERNAT, R. A. & VASCONCELOS, C. 2011. Aerobic biomineralization of Mg-rich carbonates: Implications for natural environments. *Chem Geol,* 281**,** 143-150.

SILVA-CASTRO, G. A., UAD, I., RIVADENEYRA, A., VILCHEZ, J. I., MARTIN-RAMOS, D., GONZÁLEZ-LÓPEZ, J. & RIVADENEYRA, M. A. 2013. Carbonate Precipitation of Bacterial Strains Isolated from Sediments and Seawater: Formation Mechanisms. *Geomicrobiol J,* 30**,** 840-850.

STABNIKOV, V., JIAN, C., IVANOV, V. & LI, Y. 2013. Halotolerant, alkaliphilic urease-producing bacteria from different climate zones and their application for biocementation of sand. *W J Microbiol Biotechnol,* 29**,** 1453-1460.

STALEY, B. F., SAIKALY, P. E., DE LOS REYES, F. L., 3RD & BARLAZ, M. A. 2011. Critical evaluation of solid waste sample processing for DNA-based microbial community analysis. *Biodegradation,* 22**,** 189-204.

STOCKS-FISCHER, S., GALINAT, J. K. & BANG, S. S. 1999. Microbiological precipitation of CaCO3. *Soil Biol Biochem,* 31**,** 1563-1571.

WANG, Y.-Y., YAO, Q.-Z., ZHOU, G.-T. & FU, S.-Q. 2013. Formation of elongated calcite mesocrystals and implication for biomineralization. *Chem Geol,* 360-361**,** 126-133.

XU, J., DU, Y., JIANG, Z. & SHE, A. 2015. Effects of Calcium Source on Biochemical Properties of Microbial $CaCO_3$ Precipitation. *Front Microbiol,* 6**,** 1-7.

ZAMARREÑO, D. V., INKPEN, R. & MAY, E. 2009. Carbonate crystals precipitated by freshwater bacteria and their use as a limestone consolidant. *Appl Environ Microbiol,* 75**,** 5981-5990.

Figure Legends

Fig 1. (A) Changes in the pH of the biomineralisation medium (along with a blank) during the growth of the bacteria isolated from groundwater. **(B)** Changes in the pH of the biomineralisation medium (along with a blank) during the growth of the bacteria isolated from leachate. Data points are means of experiments performed in triplicate and error bars represent the variations obtained during the pH readings.

Fig 2. Spherical calcite crystals found in solutions containing **(A)** *Bacillus licheniformis* SZH2015_A, (1) fusing of two calcite crystals. **(B)** *Bacillus pumilus* szhxjlu2015, (2) fibrous patterns on the surface of a spherical calcite crystal. **(C)** *Bacillus* sp. xjlu_herc15, (3) very small calcite crystals (<30μm) on the surface of a single calcite crystal. **(D)** *Bacillus licheniformis* adseedstjo15, (4) single spherical calcite crystal connected with non-spherical calcite crystals. **(E)** *Bacillus aerius* rawirorabr15, (5) small calcite crystals (50-75μm) fused together on the top of a calcite crystals, (6) minor cracks observed on the surface of a calcite crystals and non-spherical calcite crystal with platy overlapping layers on the surface of the calcite crystal observed in. **(F)** abiotic solution showing rhombohedral crystal forms.

Fig 3. Scanning electron micrographs showing mineral precipitates formed in the presence of *Pseudomonas nitroreducens* szh_asesj15 **(A)** Radiating growth structures in the crystal (1) and internal fusing lines on a spherical calcite crystal (2). (**B)** Arrows indicate bacterial imprints on the surface of calcite crystals formed in the presence of *Sphingopyxis* sp. szh_adharsh.

Fig 4. XRD spectra indicating multiple calcite and vaterite peaks in all five bacterial isolates and the blank. **(A)** *Bacillus licheniformis* SZH2015_A; **(B)** *Bacillus pumilus*

szhxjlu2015; **(C)** *Bacillus sp.* xjlu_herc15; **(D)** *Bacillus licheniformis* adseedstjo15; **(E)** *Bacillus aerius* rawirorabr15 and **(F)** abiotic solution. (Ca= Calcite; V= Vaterite).

Fig 5. XRD spectra showing multiple calcites and a single vaterite peak for the bacterial samples. A = *Pseudomonas nitroreducens* szh_asesj15; B = *Sphingopyxis* sp. szh_adharsh. Ca=Calcite and V=Vaterite respectively.

Fig 6. Calcium carbonate precipitation with error bars for individual bacterial solutions **(A)** *Bacillus sp.* xjlu_herc15 **(B)** *Bacillus licheniformis* adseedstjo15 **(C)** *Bacillus licheniformis* SZH2015_A **(D)** *Bacillus aerius* rawirorabr15 **(E)** *Bacillus pumilus* szhxjlu2015 **(F)** *Pseudomonas nitroreducens* szh_asesj15 **(G)** *Sphingopyxis* sp. szh_adharsh and **(H)** abiotic solution.

Table 1. Details of the 16S rRNA gene sequences retrieved from bacteria isolated from Landfill raw and fresh leachates and groundwater, respectively.

Source	Accession number	Name of bacteria	Percentage identity	Closest relative in Genbank with accession number
Landfill leachate (raw)	LC090023	*Bacillus licheniformis* SZH2015_A	98%	*Bacillus licheniformis* LRF2X (KX364925)
Landfill leachate (raw)	LC092830	*Bacillus pumilus* szhxjlu2015	98%	*Bacillus pumilus* Bp02 (KJ438145)
Landfill leachate(fresh)	LC092831	*Bacillus* sp. xjlu_herc15	97%	*Uncultured Bacillus* sp. *clone* CBHOS-08(EU371582)
Landfill leachate (fresh)	LC092832	*Bacillus licheniformis* adseedstjo15	98%	*Bacillus licheniformis* LRF2X (KX364925)
Landfill leachate (fresh)	LC092833	*Bacillus aerius* rawirorabr15	99%	*Bacillus aerius* CCMMB945(KF879282)
Landfill groundwater	LC090854	*Pseudomonas nitroreducens* szh_asesj15	98%	*Pseudomonas nitroreducens* TA-E11 (KX682023)
Landfill groundwater	LC090855	*Sphingopyxis* sp. szh_adharsh	99%	*Sphingopyxis* sp. AX-A (Jq418293)

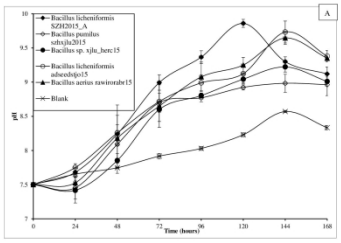

Fig 1. (A) Changes in the pH of the biomineralisation medium (along with a blank) during the growth of the bacteria isolated from groundwater. **(B)** Changes in the pH of the biomineralisation medium (along with a blank) during the growth of the bacteria isolated from leachate. Data points are means of experiments performed in triplicate and error bars represent the variations obtained during the pH readings.

Fig 1. (A) Changes in the pH of the biomineralisation medium (along with a blank) during the growth of the bacteria isolated from groundwater. (B) Changes in the pH of the biomineralisation medium (along with a blank) during the growth of the bacteria isolated from leachate. Data points are means of experiments performed in triplicate and error bars represent the variations obtained during the pH readings.

140x396mm (300 x 300 DPI)

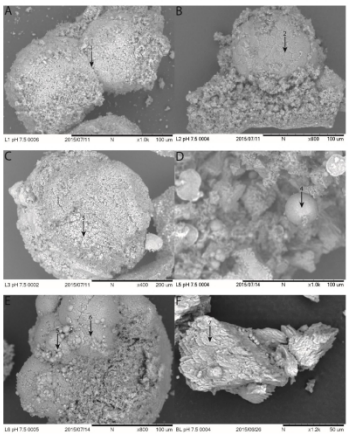

Fig 2. Spherical calcite crystals found in solutions containing **(A)** Bacillus licheniformis SZH2015_A, (1) fusing of two calcite crystals. **(B)** Bacillus pumilus szhxjlu2015, (2) fibrous patterns on the surface of a spherical calcite crystal. **(C)** Bacillus sp. xjlu_herc15, (3) very small calcite crystals(<30μm) on the surface of a single calcite crystal. **(D)** Bacillus licheniformis adseedstjo15, (4) single spherical calcite crystal connected with non-spherical calcite crystals. **(E)** Bacillus aerius rawirorabr15, (5) small calcite crystals (50-75μm) fused together on the top of a calcite crystals, (6) minor cracks observed on the surface of a calcite crystals and non-spherical calcite crystal with platy overlapping layers on the surface of the calcite crystal observed in. **(F)** blank showing rhombohedral crystal forms.

Fig 2. Spherical calcite crystals found in solutions containing (A) Bacillus licheniformis SZH2015_A, (1) fusing of two calcite crystals. (B) Bacillus pumilus szhxjlu2015, (2) fibrous patterns on the surface of a spherical calcite crystal. (C) Bacillus sp. xjlu_herc15, (3) very small calcite crystals (<30μm) on the surface of a single calcite crystal. (D) Bacillus licheniformis adseedstjo15, (4) single spherical calcite crystal connected with non-spherical calcite crystals. (E) Bacillus aerius rawirorabr15, (5) small calcite crystals (50-75μm) fused together on the top of a calcite crystals, (6) minor cracks observed on the surface of a calcite crystals and non-spherical calcite crystal with platy overlapping layers on the surface of the calcite crystal observed in. (F) abiotic solution showing rhombohedral crystal forms.

143x372mm (300 x 300 DPI)

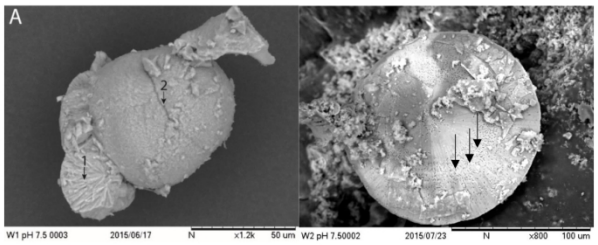

Fig 3. Scanning electron micrographs showing mineral precipitates formed in the presence of Pseudomonas nitroreducens szh_asesj15 **(A)** Radiating growth structures in the crystal (1) and internal fusing lines on a spherical calcite crystal (2). **(B)** Arrows indicate bacterial imprints on the surface of calcite crystals formed in the presence of Sphingopyxis sp. szh_adharsh.

Fig 3. Scanning electron micrographs showing mineral precipitates formed in the presence of Pseudomonas nitroreducens szh_asesj15 (A) Radiating growth structures in the crystal (1) and internal fusing lines on a spherical calcite crystal (2). (B) Arrows indicate bacterial imprints on the surface of calcite crystals formed in the presence of Sphingopyxis sp. szh_adharsh.

140x198mm (300 x 300 DPI)

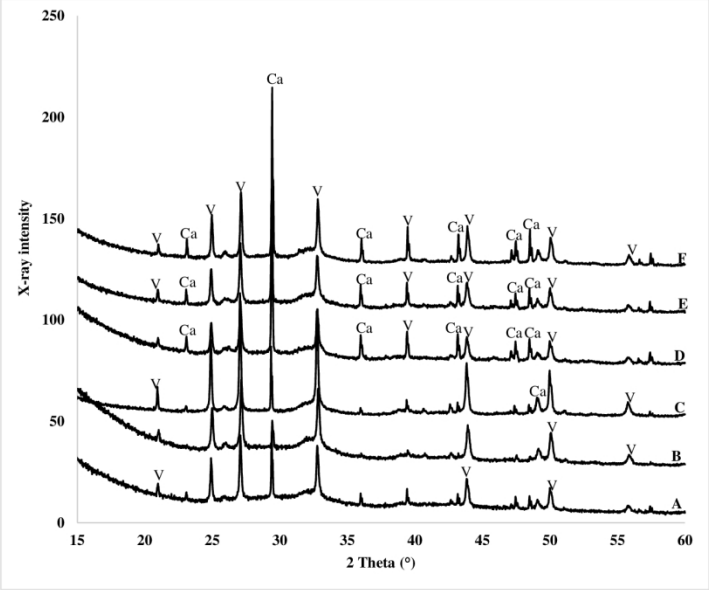

Fig 4. XRD spectra indicating multiple calcite and vaterite peaks in all five bacterial isolates and the blank. **(A)** Bacillus licheniformis SZH2015_A; **(B)** Bacillus pumilus szhxjlu2015; **(C)** Bacillus sp. xjlu_herc15; **(D)** Bacillus licheniformis adseedstjo15; **(E)** Bacillus aerius rawirorabr15 and **(F)** blank. (Ca= Calcite; V= Vaterite).

Fig 4. XRD spectra indicating multiple calcite and vaterite peaks in all five bacterial isolates and the blank. (A) Bacillus licheniformis SZH2015_A; (B) Bacillus pumilus szhxjlu2015; (C) Bacillus sp. xjlu_herc15; (D) Bacillus licheniformis adseedstjo15; (E) Bacillus aerius rawirorabr15 and (F) abiotic solution. (Ca= Calcite; V= Vaterite).

143x186mm (300 x 300 DPI)

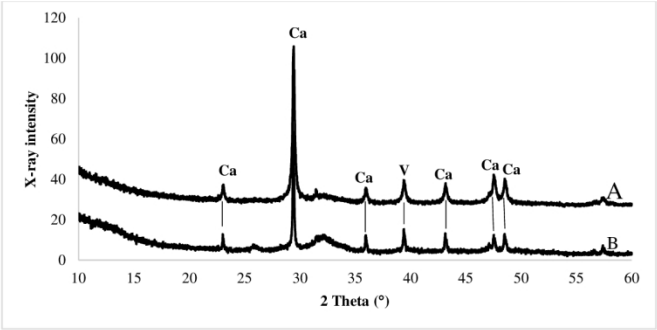

Fig 5. XRD spectra showing multiple calcites and a single vaterite peak for the bacterial samples. A = Pseudomonas nitroreducens szh_asesj15; B = Sphingopyxis sp. szh_adharsh. Ca=Calcite and V=Vaterite respectively.

Fig 5. XRD spectra showing multiple calcites and a single vaterite peak for the bacterial samples. A = Pseudomonas nitroreducens szh_asesj15; B = Sphingopyxis sp. szh_adharsh. Ca=Calcite and V=Vaterite respectively.

143x186mm (300 x 300 DPI)

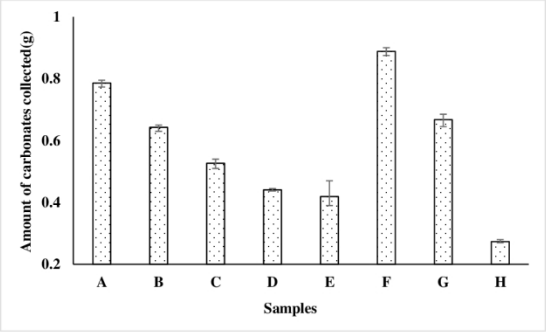

Fig 6. Calcium carbonate precipitation with error bars for individual bacterial solutions **(A)** Bacillus sp. xjlu_herc15 **(B)** Bacillus licheniformis adseedstjo15 **(C)** Bacillus licheniformis SZH2015_A **(D)** Bacillus aerius rawirorabr15 **(E)** Bacillus pumilus szhxjlu2015 **(F)** Pseudomonas nitroreducens szh_asesj15 **(G)** Sphingopyxis sp. szh_adharsh and **(H)** blank.

Fig 6. Calcium carbonate precipitation with error bars for individual bacterial solutions (A) Bacillus sp. xjlu_herc15 (B) Bacillus licheniformis adseedstjo15 (C) Bacillus licheniformis SZH2015_A (D) Bacillus aerius rawirorabr15 (E) Bacillus pumilus szhxjlu2015 (F) Pseudomonas nitroreducens szh_asesj15 (G) Sphingopyxis sp. szh_adharsh and (H) abiotic solution.

143x186mm (300 x 300 DPI)